

See discussions, stats, and author profiles for this publication at: <https://www.researchgate.net/publication/235418270>

Effect of Morphology on Ultrafast Carrier Dynamics in Asymmetric Gold–Iron Oxide Plasmonic Heterodimers

ARTICLE *in* THE JOURNAL OF PHYSICAL CHEMISTRY C · DECEMBER 2012

Impact Factor: 4.77 · DOI: 10.1021/jp309462q

CITATIONS

5

READS

48

4 AUTHORS, INCLUDING:



Kseniya Korobchevskaya

Istituto Italiano di Tecnologia

9 PUBLICATIONS 109 CITATIONS

SEE PROFILE



Chandramohan George

University of Cambridge

35 PUBLICATIONS 378 CITATIONS

SEE PROFILE



Liberato Manna

Istituto Italiano di Tecnologia

318 PUBLICATIONS 16,281 CITATIONS

SEE PROFILE

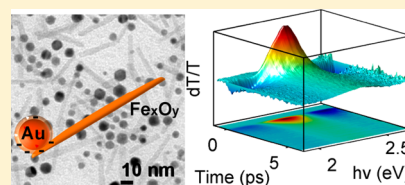
Effect of Morphology on Ultrafast Carrier Dynamics in Asymmetric Gold–Iron Oxide Plasmonic Heterodimers

Kseniya Korobchevskaya, Chandramohan George, Liberato Manna, and Alberto Comin*

Istituto Italiano di Tecnologia, via Morego 30, 16163 Genova GE, Italy

S Supporting Information

ABSTRACT: Understanding how nanoscale interfaces affect electrical and optical properties of multifunctional nanocrystal heterostructures is of paramount importance for their technological application. In this context, we investigated the ultrafast carrier dynamics of rodlike gold–iron oxide nanocrystal heterodimers, in a spectral region close to the surface plasmon resonance frequency, by means of broad-band transient absorption spectroscopy. We found that the electron–phonon relaxation time is independent of the morphology of the iron oxide domain. Moreover, we revealed a transient shift in the surface plasmon resonance frequency, which can be related to charge transfer at the interface between gold and iron oxide.



INTRODUCTION

Nanocrystal (NCs) heterostructures can combine different physical properties in one object.¹ In particular, gold–iron oxide heterodimers (HDs) contain a plasmonic and a magnetic domain and are interesting for imaging,² catalysis,³ and medicine.^{2,3} The optical properties of HDs, and specifically their absorption spectrum, depend on the size and morphology of domains, as well as on their mutual interaction.¹ The nature of interfaces is essential in determining the optoelectronic properties of nanocrystal heterostructures.⁴ For example, a different number of interface trap states, in otherwise similar HDs, is presumably the cause of the existence of two controversial reports on Au-tipped CdS nanorods.^{4,5} According to Khon et al., in these systems, plasmon–exciton coupling causes significant suppression of the gold surface plasmon resonance (SPR) and of the CdSe exciton peaks.⁵ However, Mongin et al. observed both features in a comparable sample and also found evidence for ultrafast (<20 fs) charge transfer from CdS to Au.⁴

The optical properties of core–shell nanoparticles can be described using the Mie theory,⁶ although it is not straightforward to obtain quantitative agreement with experiments. For example, Shi et al. calculated, for 2 nm iron oxide (shell)–10 nm Au (core) nanoparticles, a SPR peak at 2.12 eV (584 nm), while the measured value was 2.21 eV (560 nm).⁷ Computing the extinction spectrum of asymmetric HDs is even more challenging, and it is done numerically, for example, using the discrete dipole approximation method.⁸ In general, when a metal domain is embedded in a semiconductor shell, its plasmon resonance is broadened and red-shifted.⁹ The peak position depends on the dielectric function of the environment: the higher the dielectric function, the more red-shifted the plasmon resonance.⁹ Indeed, metal (core)–semiconductor (shell) heterostructures have significantly red-shifted plasmon peaks with respect to the corresponding metal domains.¹⁰ This effect was observed for different types of core–shells: Au–

FeOx core–shell NCs,^{7,10,11} Au-core/FeOx-hollow shell particles,¹² Au–PbS dumbbells,⁷ Au–CdSe core–shells,¹³ and Au–TiO₂ core–shells,¹⁴ and, in some cases it was also attributed to charge transfer between the domains.¹⁵ In general, charge transfer has been reported for several metal–semiconductor heterostructures. For instance, it was invoked by Xu et al. to explain the red shift of gold SPR embedded in a MgO matrix¹⁶ and by Timsen et al. in order to justify an enhancement of the catalytic properties of gold NCs deposited of α -Fe₂O₃ (hematite) platelets.¹⁷ Furube et al. observed charge transfer in Au spherical domains (10 nm), attached to TiO₂ NCs by ex situ mixing and annealing.¹⁸

Charge transfer affects the plasmonic response, because the SPR frequency is proportional to the square root of free carriers density.⁹ It is expected to have minor influence on the SPR of gold–iron oxide heterodimers (HDs) because the iron oxide domain in these HDs has numerous defect states, which can trap free electrons transferred from the gold domain.¹⁹ However, the number of defect states cannot be reliably estimated and may vary in samples with different morphologies.¹⁹ To elucidate this point, in a previous paper of our group we compared the near-IR transient absorption signals of rodlike and dumbbell-like HDs,^{11,19} made of an almost spherical gold NCs, enclosed in a asymmetric iron oxide domain (see Figure 1c, d). In those measurements, the pump and probe photon energies were 3.10 and 1.55 eV, and the contribution from the iron oxide domain dominated the time-resolved signal. Interestingly, the hot iron oxide electrons relaxed faster in rodlike HDs compared to dumbbell-like HDs, despite a thinner iron oxide coating, probably because they had more interface defects, due to the different synthesis approaches by which they were prepared.¹⁹ We therefore suggested that the observed

Received: September 24, 2012

Revised: November 1, 2012

Published: December 3, 2012



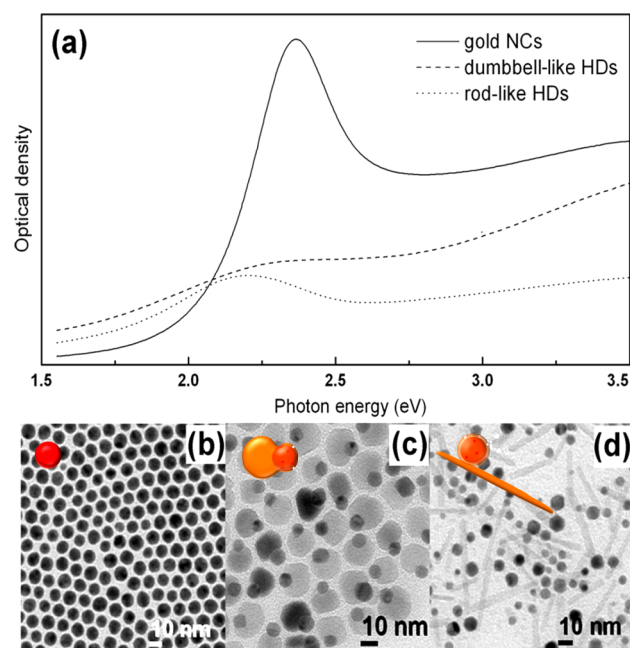


Figure 1. (a) Static absorption spectra of gold only NCs (solid line), gold–iron oxide rodlike HDs (dotted line), and gold–iron oxide dumbbell-like HDs (dashed line). TEM images of gold NCs (b), dumbbell-like HDs, and (c) and rodlike HDs (d).

dynamics could reflect charge transfer from gold to iron oxide, followed by fast trapping by defect states. A possible way to reveal changes in the density and mobility of the gold free electrons is to record transient absorption spectra near the gold SPR frequency, where the time-resolved signal appears to be dominated by the relaxation of hot electrons.¹⁰ For example, charge transfer from gold to iron oxide would red shift the SPR frequency and also decrease the electronic screening and, consequently, shorten the electron–phonon decay time.^{10,20} In our previous work on dumbbell-like HDs,¹⁰ we did not find a transient spectral shift of the SPR, which confirms the absence of charge transfer in this material. However, we still observed a faster electron–phonon relaxation in the gold domain when this was interfaced with iron oxide. We attributed this effect to spill-out of gold free electrons and trapping in the iron oxide defect states at the gold/iron oxide interface.

In the present study, we performed broad-band transient absorption spectroscopy on rodlike HDs. We found a spectral shift between the transient and static spectra, which is in line with our previous hypothesis of electron transfer from gold to iron oxide. We also show that, despite the fact that the environment of the gold domain in rodlike HDs is different from that of the dumbbell-like HDs, the hot electrons relaxation lifetime is the same in the two cases. Therefore, the decrease of the electron–phonon lifetime with respect to gold “only” NCs can be ascribed to a purely interfacial effect.

METHODS

The nanocrystals reported in this paper were synthesized following George et al.^{19,21} The morphological characterization was made by transmission electron microscopy (TEM) using a JEOL JEM 1001 microscope. TEM images for gold NCs and dumbbell-like and rodlike HDs are reported in Figure 1b–d. The static absorption spectra were recorded in toluene in 1 cm quartz cells, using a Varian Cary 5000UV–vis–NIR spec-

trometer. Transient absorption measurements were performed on a home-built pump–probe setup based on amplified Ti:sapphire laser (Coherent Micra and Legend) with the following parameters: photon energy 1.55 eV, bandwidth 60 meV, pulse duration 60 fs, repetition rate 1 kHz. The pump beam was obtained by frequency doubling on a 0.2 mm BBO crystal. The probe was a white light super continuum beam, generated by focusing a small portion of the laser output on a 3 mm sapphire plate. Spot sizes (full width half-maximum) were 1 mm for the pump and 0.5 mm for probe beam. Energy fluencies were kept relatively low (<200 $\mu\text{J}/\text{cm}^2$ for pump, 10 $\mu\text{J}/\text{cm}^2$ for probe) to avoid sample damage. The signal was detected with a linear array spectrometer (Avantes), synchronized with the laser. The samples were dispersed in toluene and loaded in 1 mm quartz cells (Hellma). The group velocity dispersion was numerically compensated for the probe beam.

RESULTS AND DISCUSSION

Figure 1 shows the transmission electron microscopy (TEM) images and the steady state absorption spectra of single gold nanocrystals (NCs), gold–iron oxide dumbbell-like HDs, and gold–iron oxide rodlike HDs. For both HDs, a thin spherical shell (about 1 nm) encloses the gold domain. This feature is hard to spot in the TEM images, but it can be recognized after leaching out the gold from the HDs (see Supporting Information). Also, from Figure 1 it can be seen that both HDs exhibited a broadened and red-shifted plasmon peak. The broadening had likely two causes: an intrinsic one, due to the dephasing of the gold conduction electrons at the interface, and an extrinsic one, due to sample inhomogeneity. Remarkably, the plasmon peak of rodlike HDs was narrower than the one of dumbbells. This could have been caused by bigger size dispersion of gold domains.²² The reason is that the extinction cross section of a nanocrystal is proportional to its volume,⁶ and bigger nanocrystals have narrower plasmonic resonances.^{9,23} On the other hand, from the previous discussion, the red shift of the SPR frequency could be explained as mainly due to a dielectric effect. However, as can be seen from the TEM images (Figure 1c,d), the average thickness of the iron oxide shell was significantly bigger for the dumbbell-like HDs. Conversely, rodlike HDs had an absorption peak at 2.2 eV (560 nm), which was more red-shifted than that of dumbbell HDs (2.3 eV, i.e., 540 nm). This result demonstrates that the average effective thickness of the shell is not the only factor that determines the SPR red shift and confirms that the electronic properties of interfaces have a significant impact on the static plasmonic response of heterostructures. It is therefore interesting to investigate whether the plasmon dynamics is affected as well.

The transient absorption spectra of gold NCs and of both types of gold–iron oxide HDs, recorded near the gold SPR frequency after the absorption of a 60 fs, 3.1 eV laser pulse, are shown in Figure 2. The pump energy fluence was 110 $\mu\text{J}/\text{cm}^2$ for gold NCs, 93 $\mu\text{J}/\text{cm}^2$ for dumbbell-like HDs, and 140 $\mu\text{J}/\text{cm}^2$ for rodlike HDs. As it is known from studies on metal nanocrystals,⁹ the general shape of the transient spectrum reflects the broadening of the plasmon peak, caused by the increase of the electronic temperature, which smears the Fermi distribution and increases the electron damping constants.^{9,24} We note that in Figure 2 the absolute intensity of the transient absorption signal was not the same for the three samples. This quantity depends on factors like pump power, absorption cross

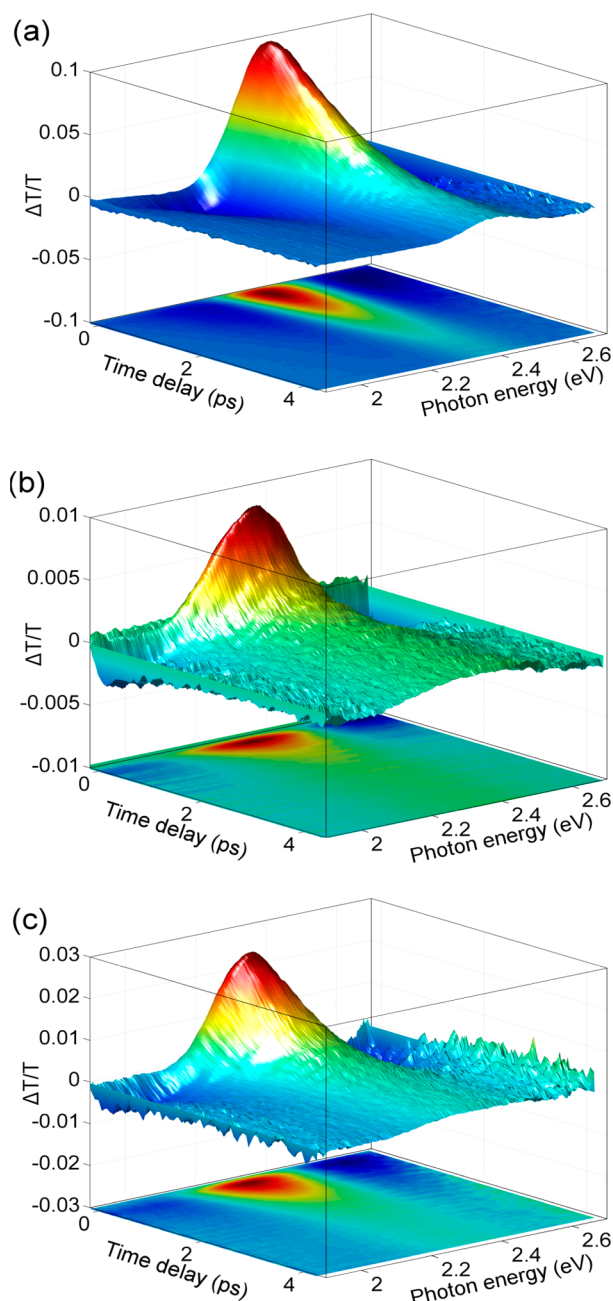


Figure 2. Transient absorption spectra of gold NCs (a), gold–iron oxide dumbbell-like HDs (b), and gold–iron oxide rodlike HDs (c) after the absorption of a 3.10 eV, 60 fs laser pulse. The pump energy fluence was $110 \mu\text{J}/\text{cm}^2$ for gold NCs, $93 \mu\text{J}/\text{cm}^2$ for dumbbell-like HDs, and $140 \mu\text{J}/\text{cm}^2$ for rodlike HDs.

section, and sample concentration. In the next paragraph we show how the involved dynamics can be understood, by analyzing a sequence of measurement at different pump powers.

In order to get a deeper insight into the hot electrons relaxation dynamics, we fitted the peak of the transient signals of rodlike HDs (2.3 eV) with a combination of two exponential decays convolved with a Gaussian kernel.²⁵ We repeated the fit for different values of the pump fluence, and we extrapolated the low power limits of the electron–electron and electron–phonon coupling time. The best-fit curves are shown in Figure 3, and, in the inset, the electron–phonon coupling times are

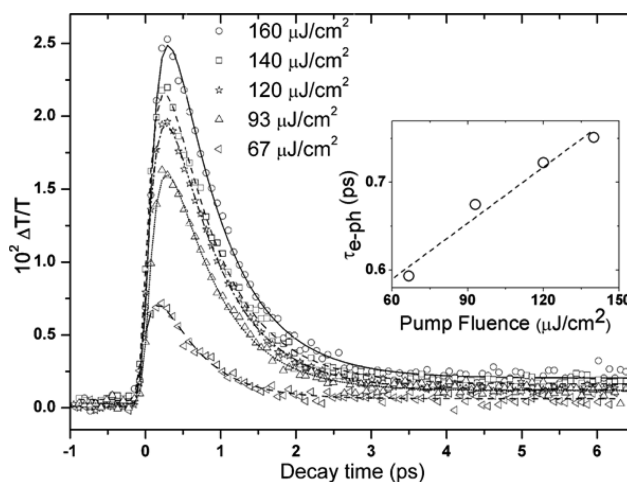


Figure 3. Transient absorption of rodlike HDs at the peak of the transient spectrum (2.3 eV) for different values of pump energy fluence. The fit curves were computed as described in the text. Inset: electron–phonon coupling time plotted as a function of the pump energy fluence and linear regression fit line.

plotted as function of pump fluence, ranging from 70 to $160 \mu\text{J}/\text{cm}^2$. A similar analysis for gold NCs and dumbbell-like HDs has been the subject of a previous publication from our group¹⁰ and serves as a comparison for the present data.

We found very similar electron–phonon decay times for dumbbell-like (0.38 ± 0.1 ps) and rodlike (0.42 ± 0.1 ps) HDs and a slower dynamics for gold-only NCs (0.7 ± 0.1 ps). This result implies that the gold plasmon dynamics is modified primarily by the presence of the interface and not much by the morphology of the iron oxide domain or by the number of interface defects, which conversely affects the carrier relaxation dynamics of the HDs in the near-infrared.¹⁹

More information can be obtained by comparing the static absorption spectra with transient spectra recorded at a fixed time delay. Figure 4 shows such a comparison for gold NCs and dumbbell-like and rodlike HDs. Here the transient spectra were recorded 0.2 ps after time 0, and the pump energy fluence was $140 \mu\text{J}/\text{cm}^2$ for gold NCs, $120 \mu\text{J}/\text{cm}^2$ for dumbbell-like HDs, and $140 \mu\text{J}/\text{cm}^2$ for rodlike HDs. The peaks of the static spectra, extracted from Figure 4a, were 2.37 ± 0.05 eV for gold NCs, 2.30 ± 0.12 eV for dumbbell-like HDs, and 2.20 ± 0.09 eV for rodlike HDs. The peaks of the transient spectra, extracted from Figure 4b, were 2.36 ± 0.02 eV for gold NCs, 2.33 ± 0.02 eV for dumbbell-like HDs, and 2.30 ± 0.03 eV for rodlike HDs. In all cases the error bars were estimated by taking the points at which the intensity dropped to 95% of the maximum. It can be recognized that, while for gold NCs and dumbbell-like HDs the static and transient peaks were almost overlapped, for rodlike HDs the positive peak of transient spectrum was shifted to higher photon energy by about 100 meV. This corresponded to a dynamic red shift of the total SPR signal (see Supporting Information). Since this effect was observed only for the rodlike HDs, but it was not evident for the dumbbell-like ones (Figure 4), we suggest that it is different from the small thermal SPR shift, which was reported before in other plasmonic NCs.⁹ The latter arises from the reduction of free carrier density that accompanies the thermal expansion of NCs, following the absorption of a laser pulse. It is illustrated for both dumbbell-like and rodlike HDs in Figure 5, which shows transient spectra recorded at a pump–probe delay of 0.2 ps, for different pump

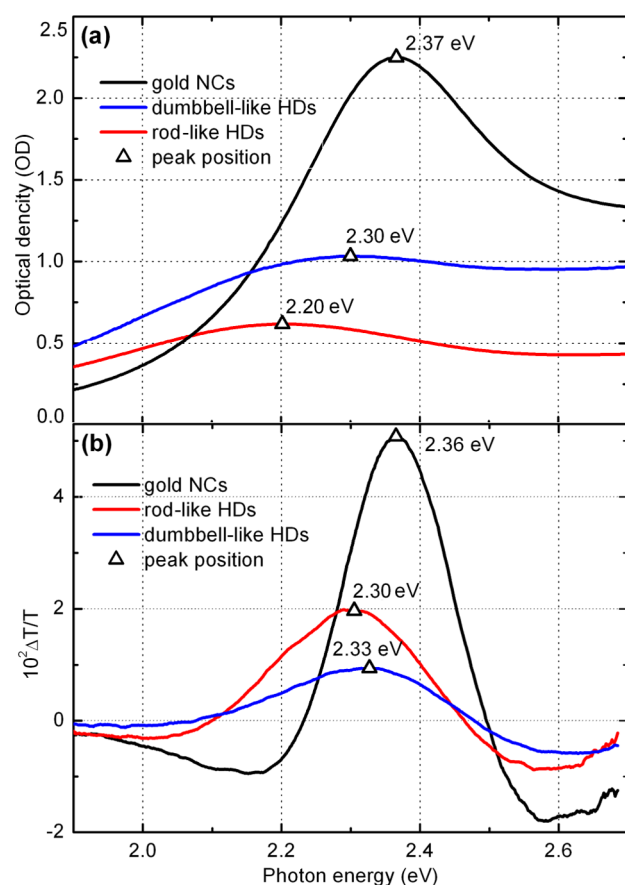


Figure 4. Static (a) and transient (b) absorption spectra of gold NCs (black), dumbbell-like HDs (blue), and rodlike HDs (red). Positions of the peaks are marked with a triangle sign. The transient spectra were recorded at a pump–probe delay of 0.2 ps; the pump energy fluence was $140 \mu\text{J}/\text{cm}^2$ for gold NCs, $120 \mu\text{J}/\text{cm}^2$ for dumbbell-like HDs, and $140 \mu\text{J}/\text{cm}^2$ for rodlike HDs.

energy fluencies (from 40 to $160 \mu\text{J}/\text{cm}^2$). As a note of caution, we remark that, due to the large inhomogeneous broadening of the spectra, our current data cannot exclude the presence of a very small transient spectral shift for the dumbbell-like HDs. This aspect could be better addressed by performing single particle measurements, which might improve accuracy in the determination of the static and transient peaks position.

According to the Mie theory, the SPR frequency is proportional to the square root of the free electron density; therefore, the observed transient frequency shift could be caused by a charge transfer process, faster than the rise time of the transient absorption signal (about 100 fs). Indeed, if the transferred carriers were quickly trapped in defect states with lifetime longer than our time window (14 ps), they could have caused a spectral shift for all probed time delays, as observed. If this hypothesis is correct, by measuring the transient absorption signal at long time delay it should be possible to observe a restoration of the SPR transient peak back to its static position, as transferred charges relax from the interfacial trap states. However, for long time delays the signal-to-noise ratio becomes too low to reliably monitor the time dependence of the SPR frequency. On a different note, simple models based on the Mie theory may not fully explain transient spectra in asymmetric gold–iron oxide HDs. For instance, justifying a 100 meV shift from a SPR peak of 2.2 eV, in the quasi-static dipole approximation, would require the assumption that about 8%

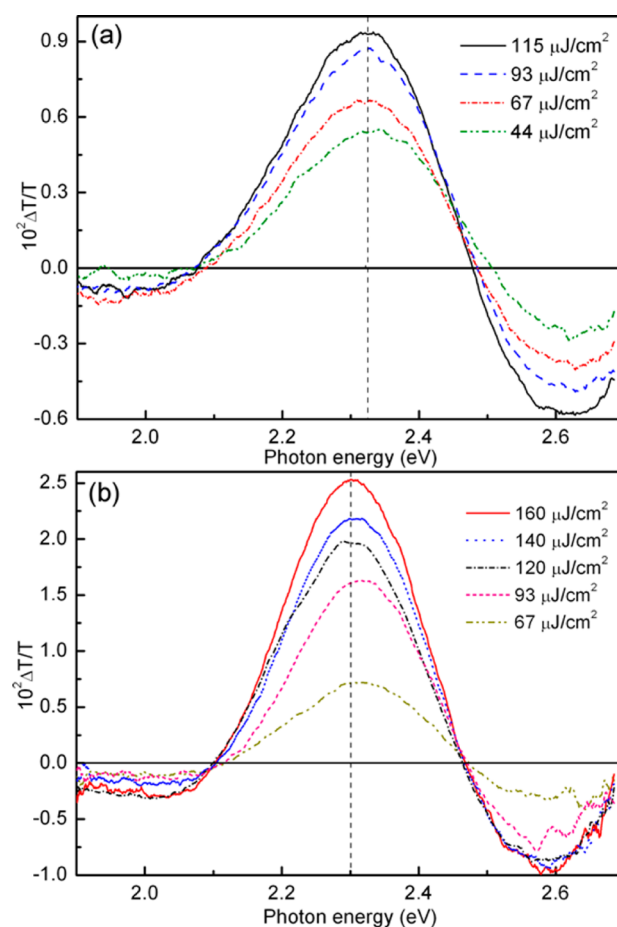


Figure 5. Transient spectra of dumbbell-like (a) and rodlike (b) HDs, recorded at a pump–probe delay of 0.2 ps, for different values of the pump energy fluence. The vertical dashed lines are drawn to better visualize the spectral shift of the SPR peak.

of the gold electrons were transferred from gold to iron oxide.¹¹ It could also be expected that such a reduction of the free electron density, caused by charge transfer, should have affected the electron–phonon coupling, making it faster for rodlike HDs than for dumbbell-like HDs,¹⁰ which is different from what we observed. It can be shown that charge transfer between gold and iron oxide not only translates the positive peak of the transient spectra, as observed, but also increases the absolute value of the negative peak in the lower energy side of the spectrum (see Supporting Information for more details). The last effect is not visible in our measurements; therefore, a more sophisticated model is required to explain the transient absorption data. One reason for the not perfect agreement with the Mie theory could be that the transferred electrons are most likely trapped in defect states near the gold–iron oxide interface, where they modify the polarizability of the interface, causing an additional dielectric shift of the SPR. On the other hand, our previous studies, performed in the near-infrared region of the spectrum, pointed to a different nature of the gold–iron oxide interface in the two types of HDs.¹⁹ In this view, the higher density of interface defect states could be responsible both for the previously reported faster carrier dynamics in the near-infrared¹⁹ and for the transient shift of the plasmon resonance observed here. In particular, given the asymmetric nature of the rodlike HDs, it could be expected that the number of trap states is higher at the interface between the

gold and the iron oxide domain. Therefore, after charge transfer and trapping into defect states, the SPR frequency would become more dependent on the polarization angle of the electric field. In our experiments, which are performed in solution, it is not possible to resolve the double peak, corresponding to the parallel and transversal configurations, also because of the inhomogeneous broadening of the SPR; however, new experiments performed at single particle level should help understand this in detail.

An alternative explanation could be that, under intense laser irradiation, the nanorods samples could have been reshaped. We excluded this hypothesis by comparing the static absorption spectra recorded before and after the time-resolved measurements. A more in-depth study would therefore be required to clarify the spectral shift between the static and time-resolved spectra of rodlike HDs. Nevertheless, our results show that this dynamic spectral shift does not influence the surface plasmon dynamics, which is affected only by the presence of iron oxide interface.

CONCLUSIONS

We studied the optical properties of two types of gold–iron oxide heterodimers: rodlike and dumbbell-like. We used broadband transient absorption spectroscopy to reveal the effect of the morphology of the iron oxide domain on the hot electrons relaxation dynamics. We found that, only for the rodlike dimers, the transient plasmon peak was clearly blue-shifted by about 100 meV with respect to the static value. The origin of this phenomenon is probably ascribable to charge transfer followed by trapping by interface states, but it will require further studies to be completely clarified. By fitting the transient absorption spectra at the surface plasmon resonance frequency, we found very similar electron–phonon decay times for dumbbell-like (0.38 ± 0.1 ps) and rodlike (0.42 ± 0.1 ps) heterodimers and a slower dynamics for single gold nanocrystals (0.7 ± 0.1 ps). This result supports the conclusion that the morphology of the iron oxide domain does not influence the hot electrons relaxation dynamics of the gold domains, but only the frequency of the surface plasmon resonance peak.

ASSOCIATED CONTENT

Supporting Information

Supplementary TEM images and detail on data analysis of transient spectra. This material is available free of charge via the Internet at <http://pubs.acs.org>.

AUTHOR INFORMATION

Corresponding Author

*Fax +39 01071781 236; tel. +39 010 71781542; e-mail alberto.comin@iit.it.

Notes

The authors declare no competing financial interest.

ACKNOWLEDGMENTS

The authors acknowledge financial support through the FP7 ERC starting grant NANO-ARCH (contract no. 240111) and the Italian Ministry of Research through the FIRB grant no. RBAP115AYN.

REFERENCES

- (1) Costi, R.; Saunders, A. E.; Banin, U. *Angew. Chem.* **2010**, *49*, 4878–4897.
- (2) Hao, R.; Xing, R.; Xu, Z.; Hou, Y.; Gao, S.; Sun, S. *Adv. Mater.* **2010**, *22*, 2729–2742.
- (3) Leung, K. C.-F.; Xuan, S.; Zhu, X.; Wang, D.; Chak, C.-P.; Lee, S.-F.; Ho, W. K.-W.; Chung, B. C.-T. *Chem. Soc. Rev.* **2012**, *41*, 1911–1928.
- (4) Mongin, D.; Shaviv, E.; Maioli, P.; Crut, A.; Banin, U.; Del Fatti, N.; Vallée, F. *ACS Nano* **2012**, *6*, 7034–7043.
- (5) Khon, E.; Mereshchenko, A.; Tarnovsky, A. N.; Acharya, K.; Klinkova, A.; Hewa-Kasakarage, N. N.; Nemitz, I.; Zamkov, M. *Nano Lett.* **2011**, *11*, 1792–1799.
- (6) Bohren, C. F.; Huffman, D. R. *Absorption and Scattering of Light by Small Particles*; John Wiley & Sons: New York, 1983.
- (7) Shi, W.; Zeng, H.; Sahoo, Y.; Ohulchanskyy, T. Y.; Ding, Y.; Wang, Z. L.; Swihart, M.; Prasad, P. N. *Nano Lett.* **2006**, *6*, 875–881.
- (8) Shaviv, E.; Schubert, O.; Alves-Santos, M.; Goldoni, G.; Di Felice, R.; Vallée, F.; Del Fatti, N.; Banin, U.; Sönnichsen, C. *ACS Nano* **2011**, *5*, 4712–4719.
- (9) Hartland, G. V. *Chem. Rev.* **2011**, *111*, 3858–3887.
- (10) Comin, A.; Korobchevskaya, K.; George, C.; Diaspro, A.; Manna, L. *Nano Lett.* **2012**, *12*, 921–926.
- (11) Korobchevskaya, K.; George, C.; Diaspro, A.; Manna, L.; Cingolani, R.; Comin, A. *Appl. Phys. Lett.* **2011**, *99*, 011907.
- (12) Shevchenko, E. V.; Bodnarchuk, M. I.; Kovalenko, M. V.; Talapin, D. V.; Smith, R. K.; Aloni, S.; Heiss, W.; Alivisatos, A. P. *Adv. Mater.* **2008**, *20*, 4323–4329.
- (13) Lu, W.; Wang, B.; Zeng, J.; Wang, X.; Zhang, S.; Hou, J. G. *Langmuir* **2005**, *21*, 3684–3687.
- (14) Choi, H.; Chen, W. T.; Kamat, P. V. *ACS Nano* **2012**, *6*, 4418–4427.
- (15) Daniel, M.-C.; Astruc, D. *Chem. Rev.* **2004**, *104*, 293–346.
- (16) Xu, J.; Moxom, J.; Overbury, S.; White, C.; Mills, A.; Suzuki, R. *Phys. Rev. Lett.* **2002**, *88*, 175502.
- (17) Thimsen, E.; Le Formal, F.; Grätzel, M.; Warren, S. C. *Nano Lett.* **2010**, *11*, 35–43.
- (18) Furube, A.; Du, L.; Hara, K.; Katoh, R.; Tachiya, M. *J. Am. Chem. Soc.* **2007**, *129*, 14852–14853.
- (19) George, C.; Genovese, A.; Qiao, F.; Korobchevskaya, K.; Comin, A.; Falqui, A.; Marras, S.; Roig, A.; Zhang, Y.; Krahne, R.; et al. *Nanoscale* **2011**, *3*, 4647–4654.
- (20) Arbouet, A.; Voisin, C.; Christofilos, D.; Langot, P.; Fatti, N.; Vallée, F.; Lermé, J.; Celep, G.; Cottancin, E.; Gaudry, M.; et al. *Phys. Rev. Lett.* **2003**, *90*, 177401.
- (21) George, C.; Dorfs, D.; Bertoni, G.; Falqui, A.; Genovese, A.; Pellegrino, T.; Roig, A.; Quarta, A.; Comparelli, R.; Curri, et al. *J. Am. Chem. Soc.* **2011**, *133*, 2205–2217.
- (22) Mendelsberg, R. J.; Garcia, G.; Li, H.; Manna, L.; Milliron, D. J. *J. Phys. Chem. C* **2012**, *116*, 12226–12231.
- (23) Voisin, C.; Christofilos, D.; Del Fatti, N.; Vallée, F.; Prevel, B.; Cottancin, E.; Lermé, J.; Pellarin, M.; Broyer, M. *Phys. Rev. Lett.* **2000**, *85*, 2200–2203.
- (24) Logunov, S. L.; Ahmadi, T. S.; El-Sayed, M. A.; Khoury, J. T.; Whetten, R. L. *J. Phys. Chem. B* **1997**, *101*, 3713–3719.
- (25) Del Fatti, N.; Voisin, C.; Achermann, M.; Tzortzakakis, S.; Christofilos, D.; Valle, F. *Phys. Rev. B* **2000**, *61*, 956–966.